

Supplementary Information For:

“Single Molecule Glycosylase Studies with Engineered 8-oxoguanine DNA Damage Sites Show Functional Defects of a MUTYH Polyposis Variant”

Shane R. Nelson^b, Scott D. Kathe^a, Thomas S. Hilzinger^{a,1}, April M. Averill^a, David M. Warshaw^b, Susan S. Wallace^a, Andrea J. Lee^{a,*}

^aDepartment of Microbiology and Molecular Genetics, Markey Center for Molecular Genetics, The University of Vermont, 95 Carrigan Drive, Stafford Hall, Burlington, Vermont 05405-0084, USA

^bDepartment of Molecular Physiology and Biophysics, University of Vermont, Health Science Research Facility, 149 Beaumont Avenue, Burlington, VT 05405-0075, USA

¹Present address: Pricewaterhouse Coopers LLP, One North Wacker Drive, Chicago, IL 60606

*To whom correspondence may be addressed. Email: Andrea.Lee@med.uvm.edu

Supplemental Methods

Protein expression and purification. The EcMuty plasmid was transformed into Rosetta2(DE3)pLysS competent cells (Novagen) and plated onto an agar plate supplemented with 50 µg/ml kanamycin and 34 µg/ml chloramphenicol. The protein was expressed using autoinduction (Studier method). From a freshly transformed plate, approximately 20 colonies were used to inoculate 1 L of Terrific Broth (Affymetrix, Inc, Cleveland, Ohio) supplemented with 50 µg/ml kanamycin and 1X 5052 autoinduction solution (0.5% glycerol, 0.05% glucose, 0.2% α-lactose). The cultures were grown in a 2.8 L Fernbach flask (Fisher Scientific, Hampton, NH) and were shaken at 20° C for approximately 60 hours. The cells were harvested and stored at -80° C.

To purify EcMuty frozen pellets were thawed on ice and resuspended in lysis buffer (20 mM Tris, pH 7.5, 300 mM NaCl, 10 mM Imidazole, 5 mM βME, 10% Glycerol and 1 tab Roche Complete EDTA Free Protease Inhibitor). The clear lysates were harvested after sonication and centrifugation. A 5 ml HisTrap HP column (GE Healthcare, Piscataway, NJ) was equilibrated in five column volumes of chelating buffer (20 mM Tris, pH 7.5, 300 mM NaCl, 10 mM Imidazole, 5 mM βME and 10% Glycerol) and the protein was loaded onto the column using an ÄKTA Purifier (GE Healthcare). The column was washed with five column volumes of chelating buffer followed by a linear gradient from 10-500 mM Imidazole in chelating buffer (20 mM Tris, pH 7.5, 300 mM NaCl, 5 mM βME and 10% Glycerol). The protein eluted at ~ 125 mM Imidazole. Based on SDS PAGE gel analysis the fractions were pooled. The protein was then diluted to a final salt concentration of 150 mM NaCl and loaded onto a 5 ml SP-FF column (GE Healthcare, Piscataway, NJ) equilibrated in FFS buffer (20 mM Tris, pH 7.5, 150 mM NaCl, 5 mM βME and 10% Glycerol). The column was washed with five column volumes of FFS buffer (20 mM Tris, pH 7.5, 150 mM NaCl, 5 mM βME and 10% Glycerol) and the protein was eluted with a 20 column volume linear salt gradient from 150 mM - 1M NaCl in FFS buffer (20 mM Tris, pH 7.5, 5 mM βME and 10% Glycerol). Protein eluted at ~400 mM NaCl. Based on SDS PAGE gel analysis fractions were pooled and dialyzed into storage buffer (20 mM Tris, pH 7.5, 250 mM NaCl, 0.5 mM EDTA, 1 mM DTT, 50% glycerol) using SnakeSkin dialysis tubing (Thermo Scientific, Rockford, IL). After dialysis protein was stored at -20° C.

The MUTYH plasmid was transformed into Rosetta2(DE3)pLysS competent cells (Novagen) and plated onto an agar plate supplemented with respective antibiotics (50 µg/ml kanamycin and 34 µg/ml chloramphenicol). A 50 ml culture of Luria Broth (LB medium) supplemented with 50 µg/ml kanamycin was inoculated from this plate with approximately 5 colonies. The culture was grown with gentle shaking at 37°C until the OD₆₀₀ reached 0.5. This culture was added to 1L of LB medium supplemented with 50 µg/ml kanamycin and 10 µM isopropyl β-D-thiogalactoside (IPTG). The culture was grown in a 2.8 L Fernbach flask (Fisher Scientific, Hampton, NH) and was shaken at 30° C for approximately 15 hours. The cells were harvested and stored at -80° C.

To purify MUTYH frozen pellets were thawed on ice and resuspended in lysis buffer (20 mM NaPO₄, pH 7.5, 300 mM NaCl, 10 mM Imidazole, 5 mM βME, 10% Glycerol and 1 tab Roche Complete EDTA Free Protease Inhibitor). The clear lysates were harvested after sonication and

centrifugation. A 5 ml HisTrap HP column (GE Healthcare, Piscataway, NJ) was equilibrated in five column volumes of chelating buffer (20 mM NaPO₄, pH 7.5, 300 mM NaCl, 10 mM Imidazole, 5 mM βME and 10% Glycerol) and the protein was loaded onto the column using an ÄKTA Purifier (GE Healthcare). The column was washed with five column volumes of chelating buffer followed by a linear gradient from 10-500 mM Imidazole in chelating buffer (20 mM NaPO₄, pH 7.5, 300 mM NaCl, 5 mM βME and 10% Glycerol). The protein eluted at ~ 125 mM Imidazole. Based on SDS PAGE gel analysis the fractions were pooled. The protein was then diluted to a final salt concentration of 100 mM NaCl and loaded onto a 5 ml Heparin HP column (GE Healthcare, Piscataway, NJ) equilibrated in heparin buffer (20 mM NaPO₄, pH 7.5, 100 mM NaCl, 5 mM βME and 10% Glycerol). The column was washed with five column volumes of heparin buffer (20 mM NaPO₄, pH 7.5, 100 mM NaCl, 5mM βME and 10% Glycerol) and the protein was eluted with a 20 column volume linear salt gradient from 100 mM - 1M NaCl in heparin buffer (20 mM NaPO₄, pH 7.5, 5 mM βME and 10% Glycerol). Protein eluted at ~400 mM NaCl. Based on SDS PAGE gel analysis fractions were pooled and dialyzed into storage buffer (20 mM Hepes, pH 7.6, 200 mM NaCl, 1 mM EDTA, 1 mM DTT, 10% glycerol) using SnakeSkin dialysis tubing (Thermo Scientific, Rockford, IL). After dialysis protein was flash frozen in liquid nitrogen and stored at -80° C.

Our standard buffers used for SM experiments are SM elongation buffer (50 mM Tris, pH 8.0, 50-150 mM potassium glutamate, and 2 mM DTT) and SM glycosylase buffer (50 mM Tris, pH 8.0, 50-150 mM potassium glutamate, 1 mg/mL BSA and 2 mM DTT). The potassium glutamate concentrations during imaging differ for MutY (150 mM) and MUTYH (50 mM) because MUTYH Y150C shows little glycosylase activity above 50 mM NaCl. Furthermore, gel-based assays of MUTYH were carried out at 30 mM potassium glutamate for comparison with previous work (1). DTT was always freshly prepared from solid DTT on the day of imaging.

Burst phase analysis was also used to ensure that conjugation to Qdot did not affect activity of MutY WT and MUTYH WT enzymes (Fig. S11). Briefly, multiple turnover timecourse assays were carried out exactly as described above after conjugation of MUTYH or MutY with an anti-pentahistidine biotin antibody (Qiagen)/streptavidin-coated Qdot655 (Invitrogen) complex (Fig. 1c). The final molar ratio is 1 enzyme: 5 antibodies: 1 Qdot and is the same as used for imaging in the presence of lambda DNA (see below) (2). The final concentrations in the assay are 2 nM active enzyme and 20 nM A:OG 35-bp substrate. The 35-bp substrate differs in sequence from that of the 39-bp oligonucleotide describe below. The 35-bp substrate has the sequence: 5'-TGTC AATAGCAAG(damage)GGAGAAGTCAATCGTGAGTCT-3'. The complement from which the base is excised by MutY/MUTYH is 5'-AGACTCACGATTGACTTCTCCA CTGCTATTGACA-3'. Assays of Qdot-conjugated and unconjugated proteins were carried out side-by-side from the same exact thawed enzyme aliquot to ensure parity.

Single-molecule Substrates. Undamaged λ-DNA was obtained from New England Bio Labs and used as received for the “undamaged lambda” experiments. To produce abasic sites, λ-DNA was incubated at 100 ng/μl in 10 mM citrate pH 4.5 and 100 mM NaCl at 70°C for 15 minutes (3). The DNA was quickly transferred to ice, and the DNA was ethanol precipitated. The AP sites were reduced (and stabilized) by incubation for one hour at room temperature in 400 mM

Tris pH 7.8 and 5 M sodium NaBH₃CN (CAUTION! Carry out in an open container in a well-ventilated hood in case of H₂ gas evolution) (4). The λ-DNA was then dialyzed against 250 ml 10 mM Tris pH 7.8, 1 mM EDTA for 24 hours. The number of rAP sites per λ-DNA was determined by a plasmid relaxation assay (2) (Fig. S3). In this assay, pBR322 plasmid (NEB) is treated with the low pH citrate buffer described above to create AP sites. The citrate reaction is quenched at various timepoints. Damaged plasmid, 1 μg, was then incubated with 10 units of endonuclease IV (EndoIV) at 37°C for 30 min to create nicks at AP sites. Nicked plasmid was separated from supercoiled on a 1% agarose gel, the DNA bands were visualized using SybrSafe Green staining, and the fraction nicked was quantified using Quantity One Software (Bio-Rad). By plotting the fraction nicked plasmid as a function of incubation time with citrate buffer, the rate of damage production could be determined (Fig. S3) from the Poisson distribution $n = -\ln e$ where e is the ratio supercoiled sites to circular and linear forms of plasmid. These fits predicted that a 15-minute incubation with citrate produces 30 randomly located rAP sites generated per λ-DNA molecule.

The site for insertion of the damage was chosen to be directly opposite the Bsal restriction site in pUC19 which would allow the damage to lie in the center of a linearized form of the plasmid (Fig. S4). In the current study, four pNIKCAT plasmid monomers were constructed (undamaged, 8-oxoG:A, 8-oxoG:C and Cy5 dye labeled), and all plasmid identities were confirmed by sequencing before oligo insertion (UVM Advanced Genome Technology Core). For the undamaged pNIKCAT concatemer a G:C pair is used in the place of the damage site. The sequence of the undamaged 39 bp oligo is (5'-TGCATGCGGCCGCTCTTCCCATGGTGGCGATCGCTCTTCG-3', IDT), and the sequence of the complementary region in the plasmid is (5'-CGAAGAGCGATCGCACCATGGGAAGAGCGGCCGCATGCA -3'). For the 8-oxoG:A pNIKCAT, the sequence of the 39 bp oligo is (5'-TGCATGCGGCCGCTCTTCCCAT(**8-oxoG**)GTGCGATCGCTCTTCG-3', Midland), and the sequence of the complementary strand in the plasmid is (5'-CGAAGAGCGATCGCAC**A**TGGGAAGAGCGGCCGCATGCA -3'). For the 8-oxoG:C pNIKCAT, the identical 8-oxoG containing oligo was inserted into a plasmid that contained a cytosine (C) opposite the damage position. A dye marked pNIKCAT plasmid was created that contained a Cy5 dye at the damage position. The sequence of the 39 bp oligo for Cy5 pNIKCAT is (5'-TGCATGCGGCCGCTCTT*i*Cy5/CCCATGGTGGCGATCGCTCTTCG-3', IDT), and the complementary sequence in the plasmid is (5'-CGAAGAGCGATCGCACCATGGGAAGAGCGGCCGCATGCA -3').

The insertion efficiency for the 39mer was determined to be ~90% using two methods. The first method was concatemerization (described below) of 100% Cy5 labeled pNIKCAT and combing the DNA on polystyrene surfaces (Fig. S6A) (5,6). The second method was digestion of the 8-oxoG:A pNIKCAT plasmid with MUTYH and APE, followed by separation on an agarose gel to determine the fraction of plasmids that had been nicked by the BER enzymes (Fig. S5C) similar to the plasmid relaxation assays described above. Note: the “undamaged pNIKCAT” plasmid has undergone all of the steps including insertion of an undamaged 39mer oligo, removal of nonspecific damage, and purification that were utilized for the preparation of 8-oxoG:A pNIKCAT plasmid.

The concatemers vary in length, but several are very long (>15 μm in length, or 16 plasmids, as is visible in the SM image in Fig. S6B). Since Bsal cleaves in a non-palindromic region, plasmids concatemerize in one orientation with all of the damage sites on one strand of the DNA. The distance between neighboring damage sites is 2727 base pairs. To confirm this distance, the average distance between oligo insertion sites in concatemerized plasmids was measured by imaging concatemer tightropes consisting of 100% Cy5 labeled 39mer oligo inserts (Fig. S6B). These Cy5 pNIKCAT concatemers were strung up and imaged using identical conditions to those used when imaging glycosylases in the presence of Cy5-pNIKCAT containing concatemers (see below). The images were integrated over 30s and background was subtracted using the built-in ImageJ plugin with a rolling ball of 5 pixel radius. The positions of the dyes were then determined by Gaussian fit to the intensity profile across the DNA molecule (Fig. S6C).

Single-molecule Chamber Preparation. A flow chamber for microscopy was constructed from a glass slide drilled with two holes to allow for perfusion with buffers, an adhesive gasket, and a PEG-coated glass coverslip which serves as the imaging surface (Fig. 1). The chamber was blocked in 5 mg/mL casein for one hour and then rinsed with single-molecule elongation buffer (50 mM Tris, pH 8.0, 50-150 mM potassium glutamate, and 2 mM DTT) before addition of any single-molecule reagents. 3 μm silica beads were coated with poly-lysine by shaking overnight at room temperature in a solution of 0.35 $\mu\text{g}/\mu\text{L}$ polylysine in 1 M Tris, pH 8.0. Polylysine serves as an ionic site for stable non-specific adhesion of DNA tightropes. The beads were briefly spun to remove excess polylysine and then rinsed and resuspended in single-molecule elongation buffer before introduction into the chamber. The chamber was monitored during addition of the beads using an optical microscope with a 10X objective to ensure appropriate density. The chamber was then rinsed again with single molecule elongation buffer and attached to a syringe pump (Harvard) to allow for flow stretching of DNA (Fig. 1C).

Image Acquisition. For images of glycosylases on lambda substrates, a custom built TIRF microscope (Nikon TE2000) utilizing through-the-objective (PlanApo 100x, 1.49 n.a.) excitation light from a 488 nm 50 mW Argon-ion laser (Spectra-Physics, Santa Clara, CA) was used as previously described (2,7). The excitation light was adjusted to a sub-critical angle and defocused at the edge of the objective's back aperture, generating an obliquely angled illumination ray. For dual-color imaging of the Qdot-labeled glycosylases and the YOYO-1 dyed λ -DNA, the emitted light was passed through a beam splitter (Optical Insights, Pleasanton, CA) and detected using an intensified CCD camera (XR Mega-S30) running Piper Control v2.3.14 software (Standard Photonics, Stanford, CA). Image stacks of 1000 frames were captured at 15 frames/second.

Not all pauses detected in the SM displacement trajectories occur in a known position of 8-oxoG:A damage site, likely because the plasmid substrates contain a small amount of randomly occurring, off-site, residual damage (such as AP sites) that is recognized by MUTYH. The enzyme also shows a very moderate level of binding affinity for the Cy5 dye site, which are incorporated at a frequency of 20% of the available 8-oxoG:A sites. Other types of damage sites such as AP sites are present in all concatemers but are rare based on agarose gel characterization of MUTYH cleavage of plasmid starting material (Fig. S). The striking

difference between pause duration observed for MUTYH WT on 8-oxoG:A damage site (Fig. 2G) as compared with paused states in MUTYH WT on undamaged concatemer (Fig. 2A) and MUTYH Y150C on 8-oxoG:A damage site (Fig. 2J) would suggest that these slight levels of background damage site recognition do not significantly contribute to false positive interpretation of 8-oxoG-based damage site recognition behavior.

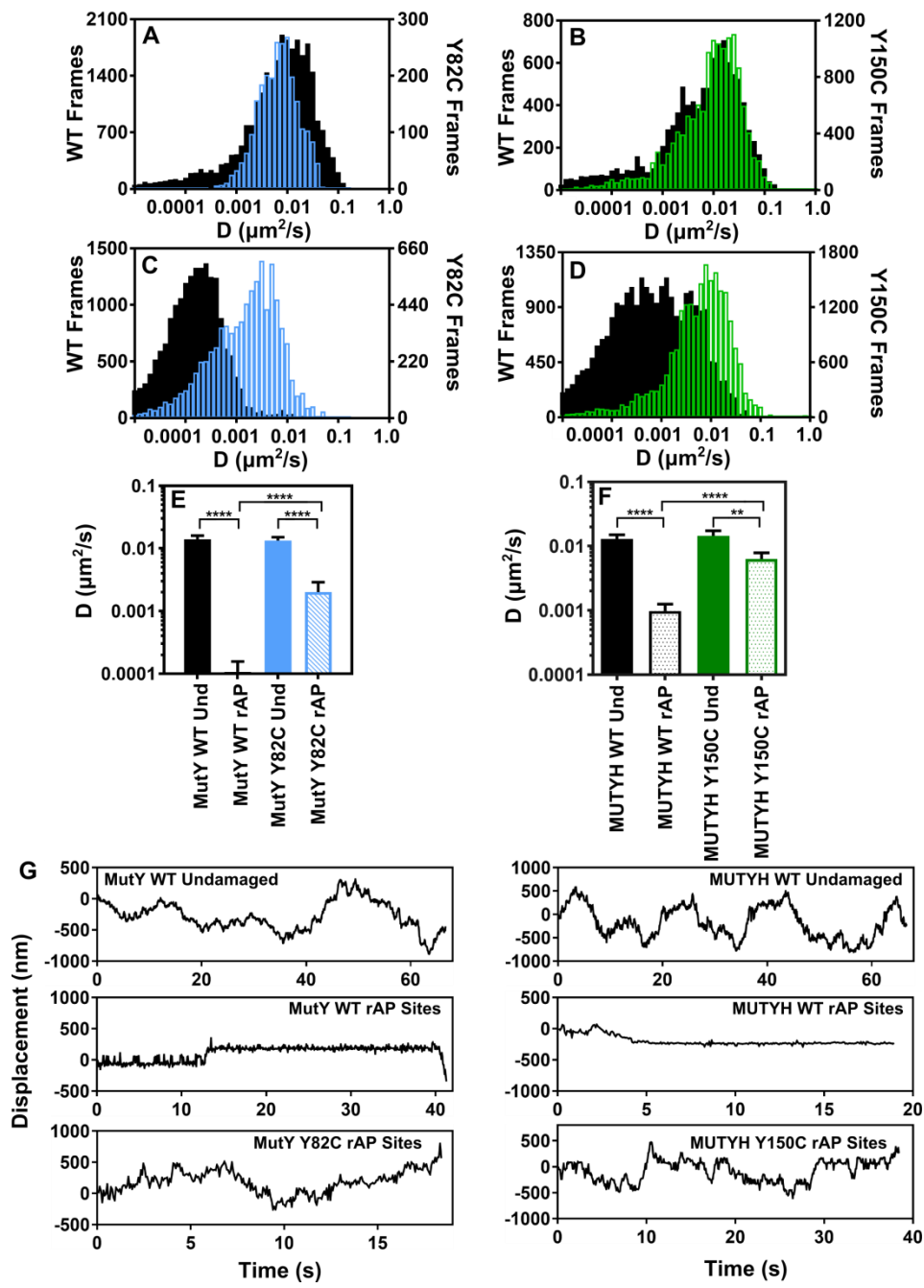


Fig. S1. Diffusion of MutY and MUTYH and wedge variant enzymes on λ DNA. Time-weighted distributions of diffusion constants from sliding window (60 frames per window) analysis of displacement trajectories for diffusion of (A) MutY WT (black bars) and MutY Y82C (blue bars) along undamaged λ DNA, (B) MUTYH WT (black bars) and MUTYH Y150C (green bars) along undamaged λ DNA, (C) MutY WT (black bars) and MutY Y82C (blue bars) λ DNA that contains ~30 randomly distributed reduced AP sites per molecule, (D) MUTYH WT (black bars) and MUTYH Y150C (green bars) along λ DNA that contains ~30 randomly distributed reduced AP sites per molecule. (E) and (F)

Mean value of diffusion constants for trajectories, determined by fitting the first 25% of the MSD plot for each trajectory (error bars represent SEM). (**** $p < 0.0001$, two tailed)
(G) Selected displacement trajectories on lambda DNA substrates.

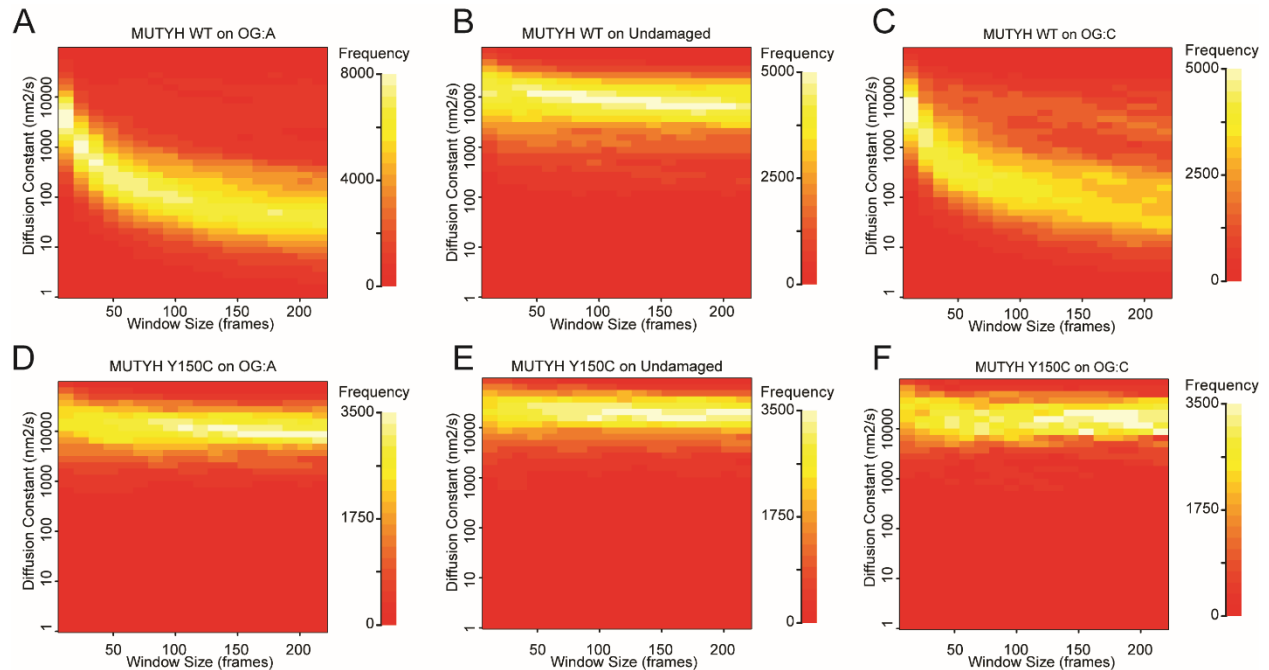
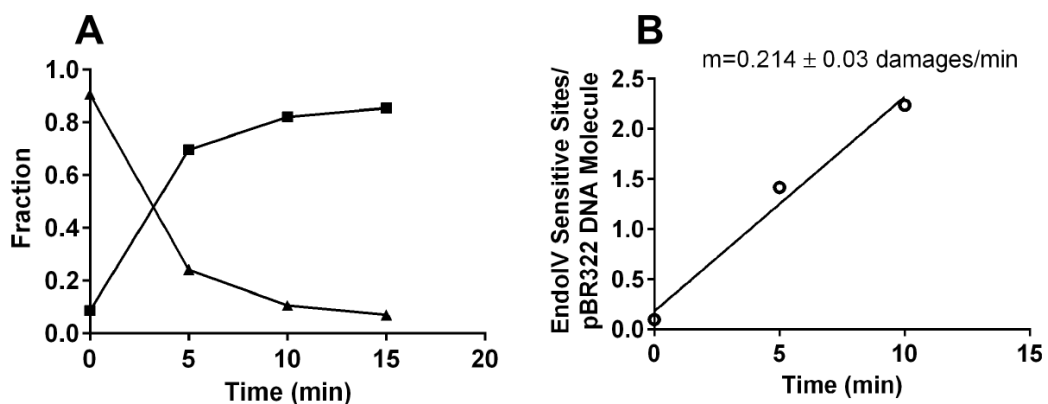


Fig. S2. Selection of Window Size for Sliding Window MSD Analysis of SM Trajectories. Tracking error contributes to apparent non-zero diffusion constants for stationary particles. However, the contribution of the tracking error is averaged out with increasing window size. (A) 2D histogram showing that as sliding window size is increased from 12 to 216 frames, the apparent diffusion constant of the predominantly stationary MUTYH WT on OG:A decreases by 2 orders of magnitude - from $0.003651 \mu\text{m}^2/\text{s}$ to $0.000037 \mu\text{m}^2/\text{s}$, respectively. However in (B), window size has minimal effect on the apparent diffusion constant of the predominantly diffusive MUTYH WT on Undamaged substrate. (C) for MUTYH WT on OG:C, similar pausing behavior is apparent, although with larger window sizes, a minor, mobile population emerges with window sizes > 100 frames. (D-F) show that window size has a negligible effect on the apparent diffusion constant of MUTYH Y150C, regardless of the substrate. Therefore, increasing window size increases the ability to differentiate pausing from diffusive behavior. However, larger window sizes prevent analysis of trajectories that are shorter than a given window size, which is particularly problematic with MUTYH Y150C (see Fig. 4). As a compromise, a 60-frame (4 second) window was selected for analysis, as this balances the ability to resolve paused and diffusive states, while minimizing the number of trajectories that must be omitted from this analysis. In the condition with the shortest trajectory lifetime (MUTYH Y150C on Undamaged substrate), this precludes analysis of 33% of the trajectories.



Figure

Fig. S3. Number of AP sites produced in λ -DNA. (A) Time dependence of EndoIV nicking of pBR322 after exposure to 10 mM citrate pH 4.5 and 100 mM NaCl at 70°C. 1 μ g of damaged pBR322 was incubated with 10 units of EndoIV for 30 minutes at 37°C. The concentration of the nicked vs. supercoiled versions of the plasmid were measured using spot densitometry (squares represent nicked plasmid, while triangles represent closed circular plasmid). (B) Rate of accumulation of AP-sites in the plasmid. The slope of the line was used to estimate the number of reduced AP sites in λ -DNA after exposure to 10 mM citrate pH 4.5 and 100 mM NaCl at 70°C for 15 minutes.

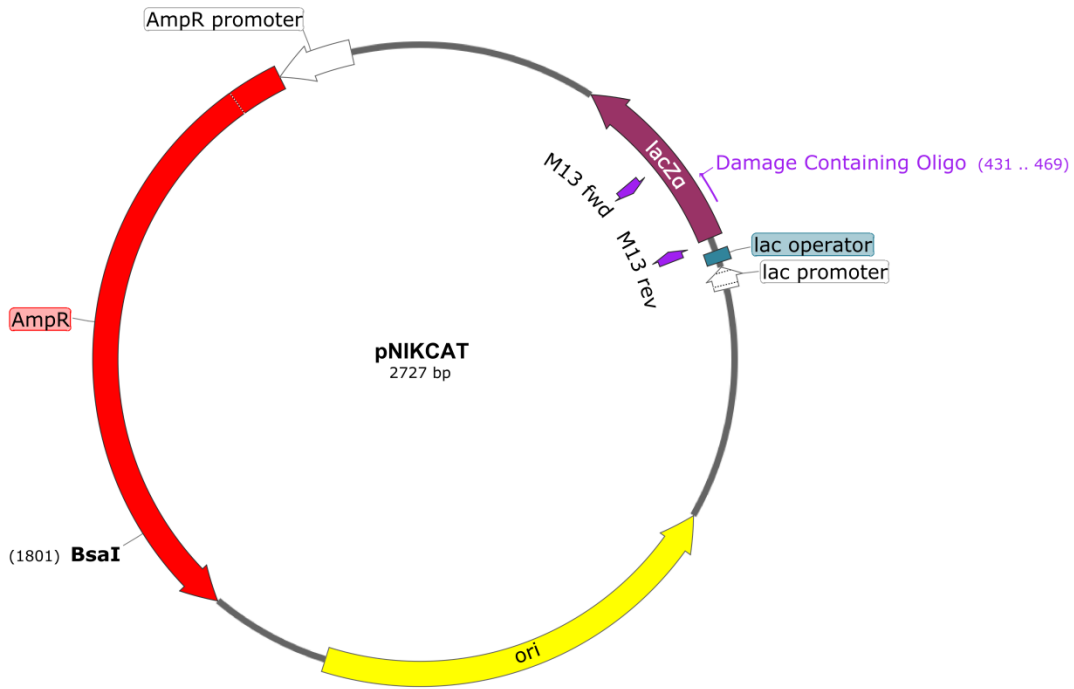


Fig. S4. Plasmid map for pNIKCAT. Plasmid map created with Snapgene program (<https://www.snapgene.com/>)

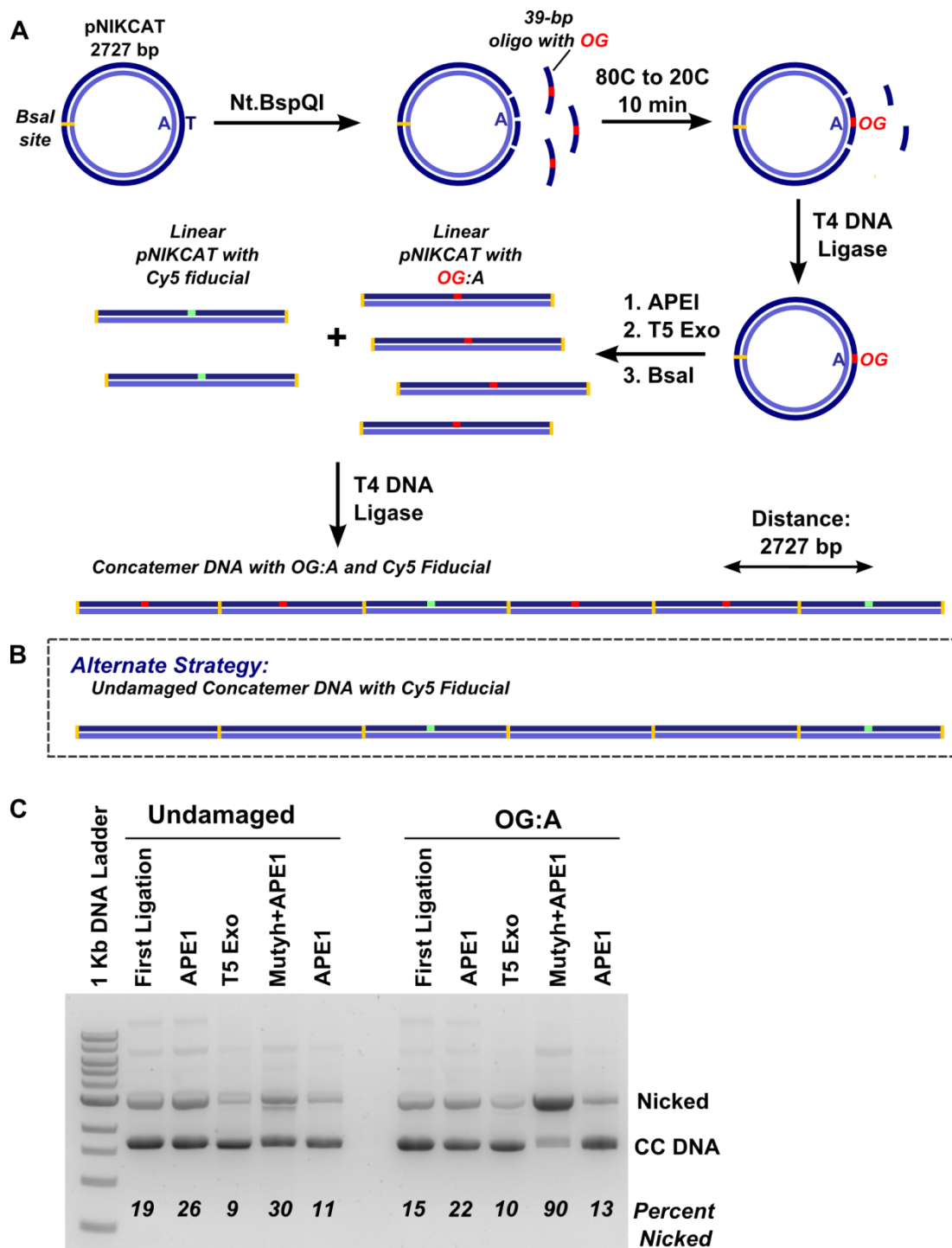


Fig. S5. Construction of plasmid concatemer DNA. (A) Steps for insertion of an oligonucleotide and concatemerization of the substrate. A parent plasmid containing an A:T pair opposite a BSA restriction site is nicked in three places with Nt.BspQI on the strand opposite the A residue. The plasmid is heated to 80C and reannealed in the presence of a 10-fold excess of 39-bp oligo containing an 8-oxoG residue that sits opposite the parental A residue. The 39-bp oligonucleotide is ligated into the plasmid before the plasmid is treated with APE to remove randomly occurring apurinic sites.

Any nicked plasmids are removed by treatment with T5 Exonuclease before the plasmid is linearized by Bsal. Linear plasmids are then concatemerized with T4 DNA ligase and damages are spaced 2727 bp apart, or ~927 nm. This procedure has been used to insert an undamaged 39-bp oligonucleotide containing a G:C pair, as well as to insert a Cy5-labeled 39-bp oligonucleotide to serve as a fiducial marker for the damage site. For microscopy experiments in the presence of specific damage, concatemers containing 20% Cy5 plasmid and 80% OG:A plasmid were constructed. (B) For microscopy experiments in the absence of specific damage, concatemers containing 30% Cy5 plasmid and 70% undamaged plasmid were constructed. (C) Agarose gel showing the fraction of nicked to closed circular plasmid at various stages of the construction process outlined in (A) for a plasmid that has an undamaged 39-bp oligo inserted and a plasmid that has OG:A 39-bp oligo inserted. The stages tested include: after insertion of the 39-bp oligo and ligation with T4 endonuclease, after treatment with APE to remove randomly occurring apurinic sites, after digestion of nicked plasmids with T5 exonuclease. The final plasmid was tested with Mutyh/APE1 and APE1, which should create nicks at OG:A and apurinic sites, respectively, to determine final concentration of enzymatically viable sites. Percent nicked plasmid is listed at the bottom of each lane.

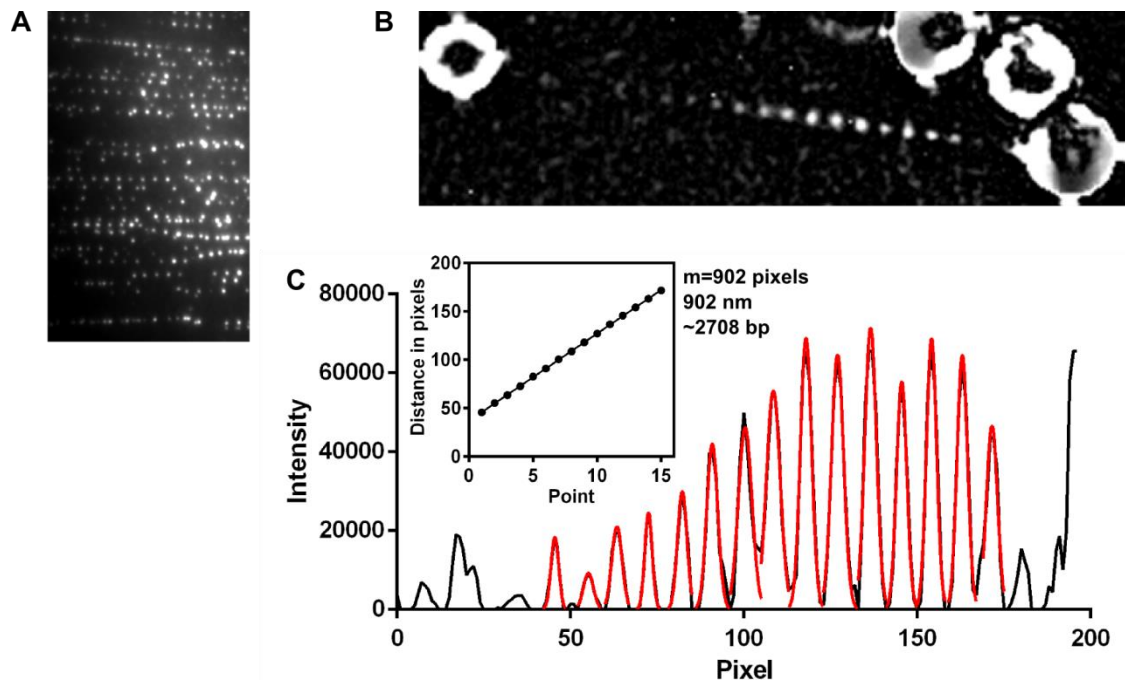


Fig. S6. Characterization of plasmid concatemer substrates. (A) 100% Cy5 pNIKCAT concatemers combed onto a polystyrene surface showing >80% yield oligonucleotide insertion into the pNIKCAT plasmid. (B) Image of 100% Cy5 pNIKCAT concatemers strung between beads in the SM TIRFM tightrope assay. This image is a z-projection of a 1000-frame image stack taken at 15 fps using 639 nm excitation. The dyes were visualized using the built-in background subtraction tool in ImageJ with a 5 pixel radius. (C) Gaussian fits of the positions of the dyes in image (B). The inset of (C) shows the linear fit of inter-dye distance gives an average separation of 2708 bp, only slightly smaller than the expected length of 2727 bp.

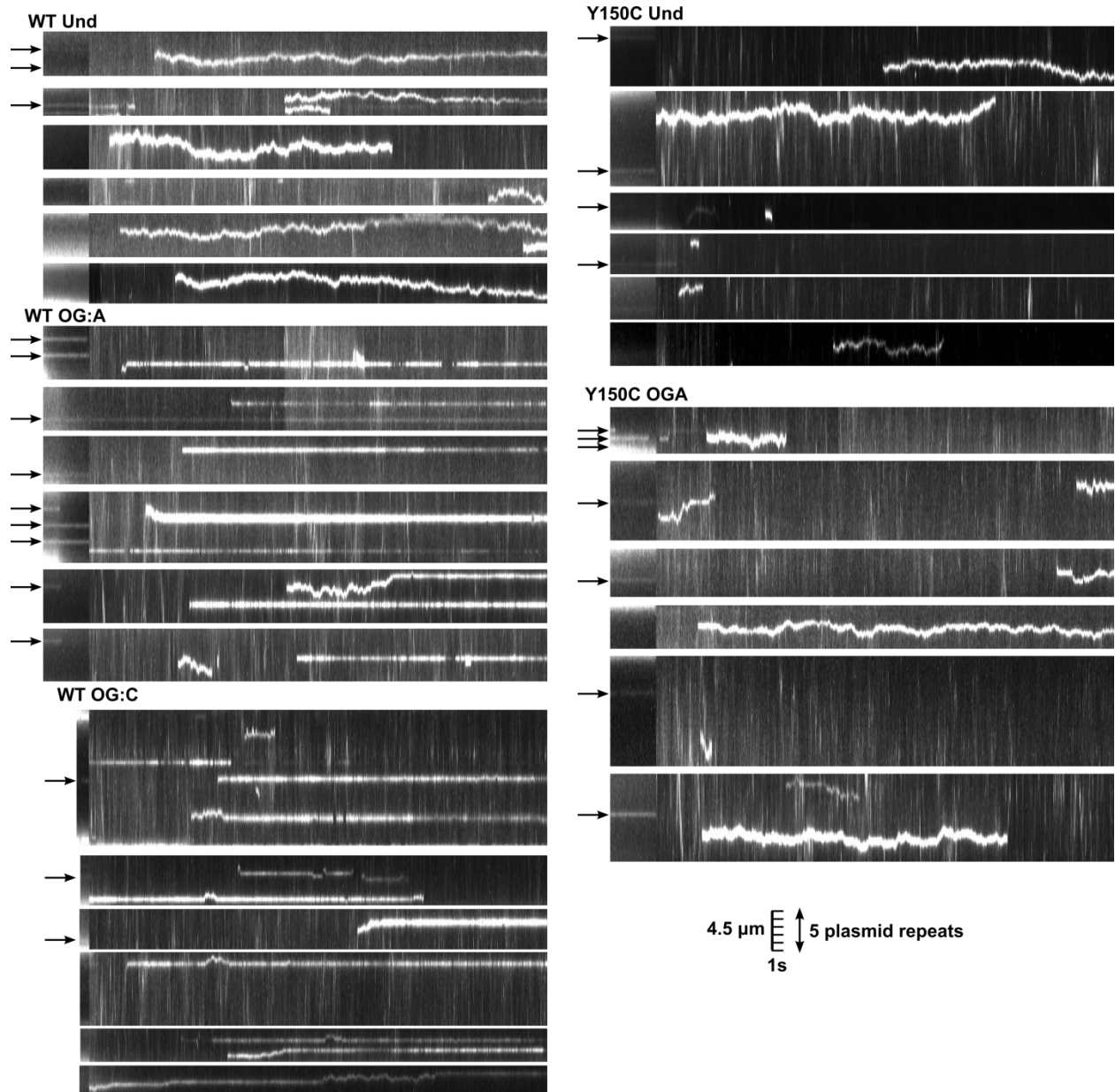


Fig. S7. Representative kymographs of MUTYH WT and Y150C scanning trajectories on various DNA concatemer substrates. The first portion of each kymograph shows the location of dye markers, which are indicated by an arrow. A scale for plasmid repeat distance is shown in the lower right and is consistent among all kymographs. Note, the dye map movie for the MUTYH WT on 8-oxoG:C was collected for a shorter duration than the other conditions, which makes the kymographs appear shorter in width.

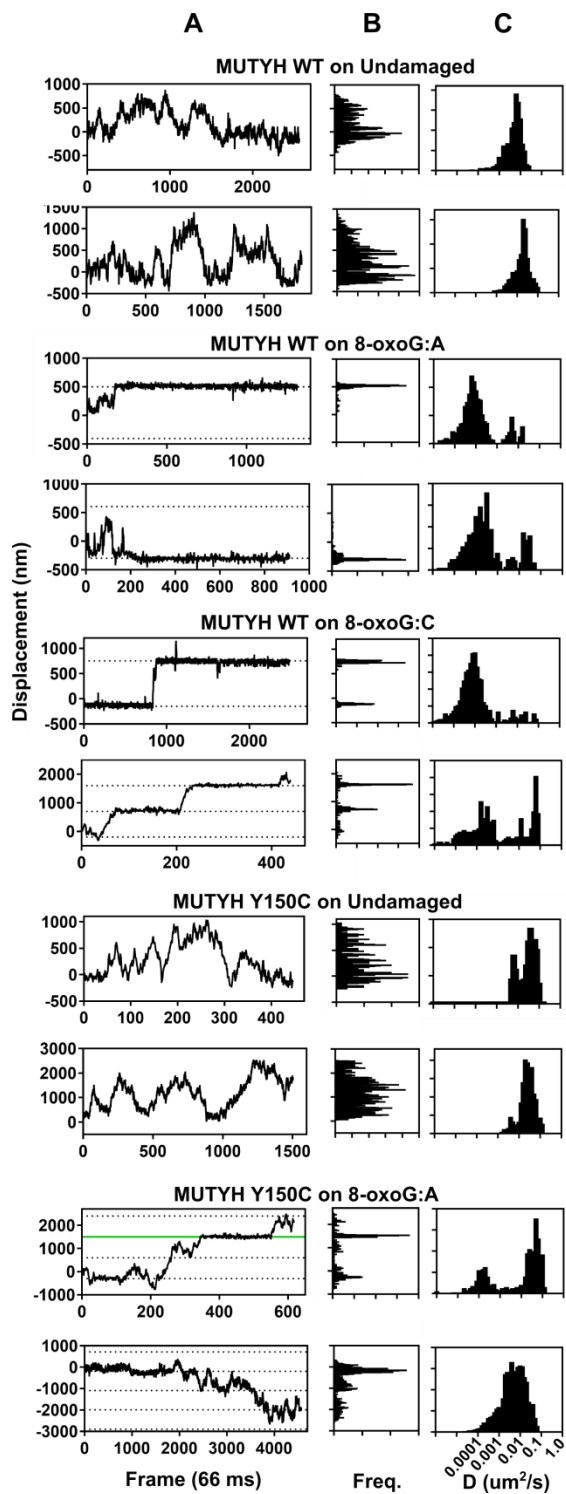


Fig. S8. Sample trajectories from SM traces of MUTYH WT and Y150C on concatemer substrates. Column A shows the Spot Tracker displacement trajectory for a representative single glycosylase in the presence of a concatemer substrate. Column B shows a histogram of how frequently a given position along the tightrope is occupied by the molecule from Column A. The scale of the y-axis in B is the same as in A. Column C shows a histogram of the diffusive behavior for the individual molecule shown in Column A.

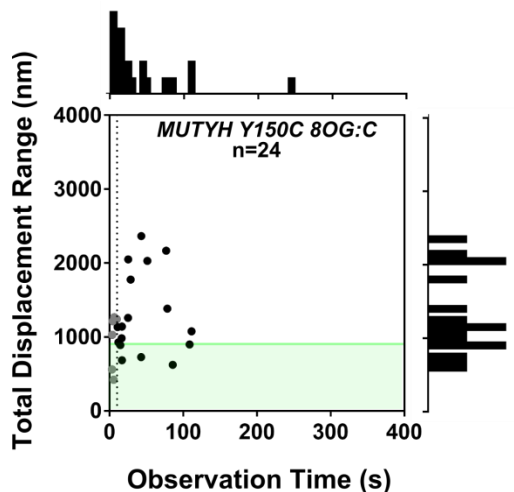


Fig. S9. Total scanning range of MUTYH Y150Con 8oxoG:C containing concatemer substrates. The total scanning range (total range of DNA scanned at least once) is plotted as a function of how long the glycosylase was observed. The dotted line corresponds to a scanning time of 10s. Gray points represent scanning events that persist for less than 10s, which were excluded from subsequent analysis. A histogram of the time observed is shown above the plot, and a histogram of total scanned range of molecules that scanned for longer than 10s is to the right of each plot. The shaded green region represents a total displacement less than the length of one plasmid concatemer.

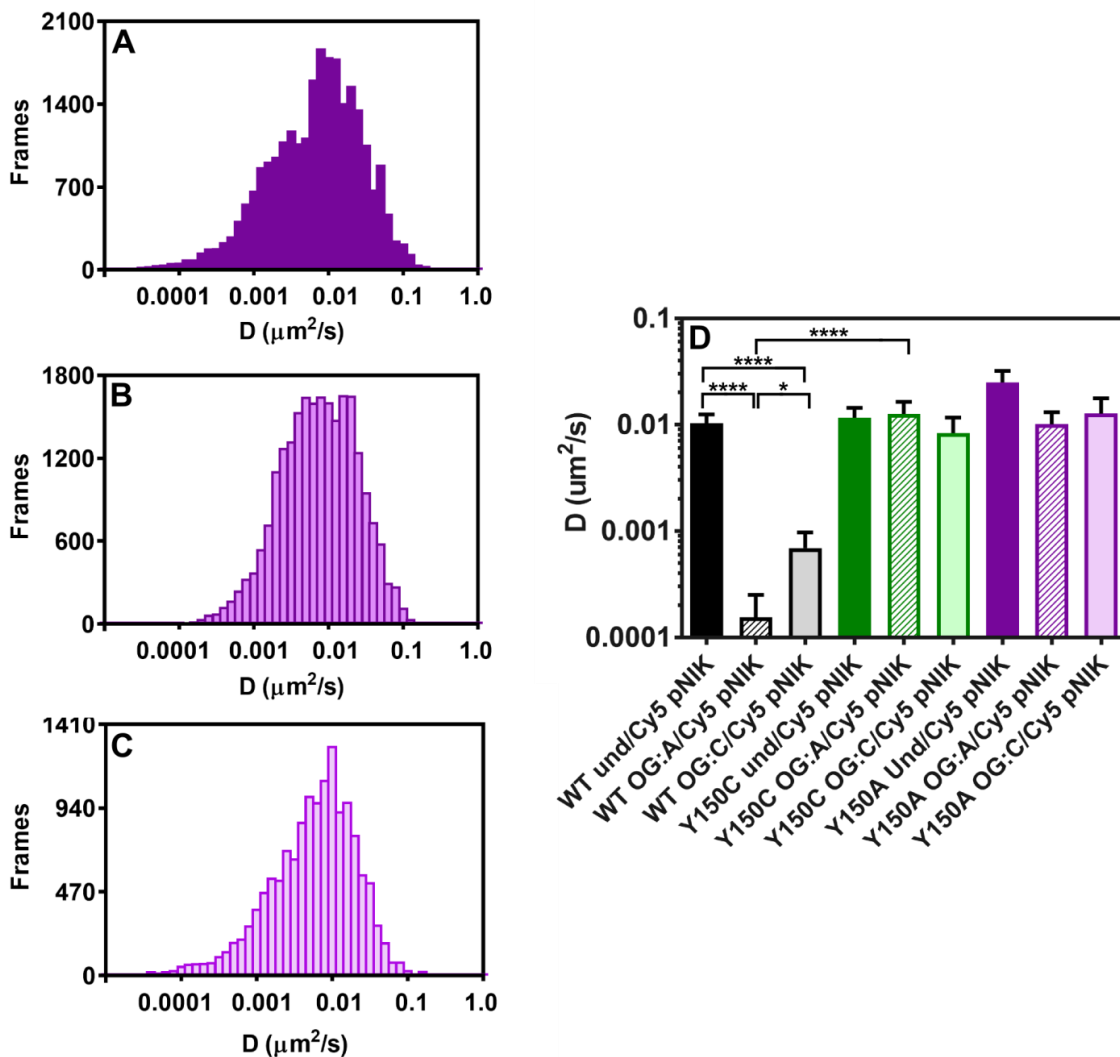


Fig. S10. Diffusion Behavior of MUTYH Y150A along concatemer tigtropes. Time-weighted distributions of diffusion constants from sliding window (60 frames per window) analysis of displacement trajectories for diffusion of MUTYH Y150C on (A) undamaged, (B) 8-oxoG:A, and (C) 8-oxoG:C. (D) Mean value of diffusion constants for trajectories, determined by fitting the first 25% of the MSD plot for each trajectory (error bars represent SEM). (**** $p < 0.0001$, two-tailed) MUTYH WT and MUTYH Y150C are included in panel (D) for comparison.

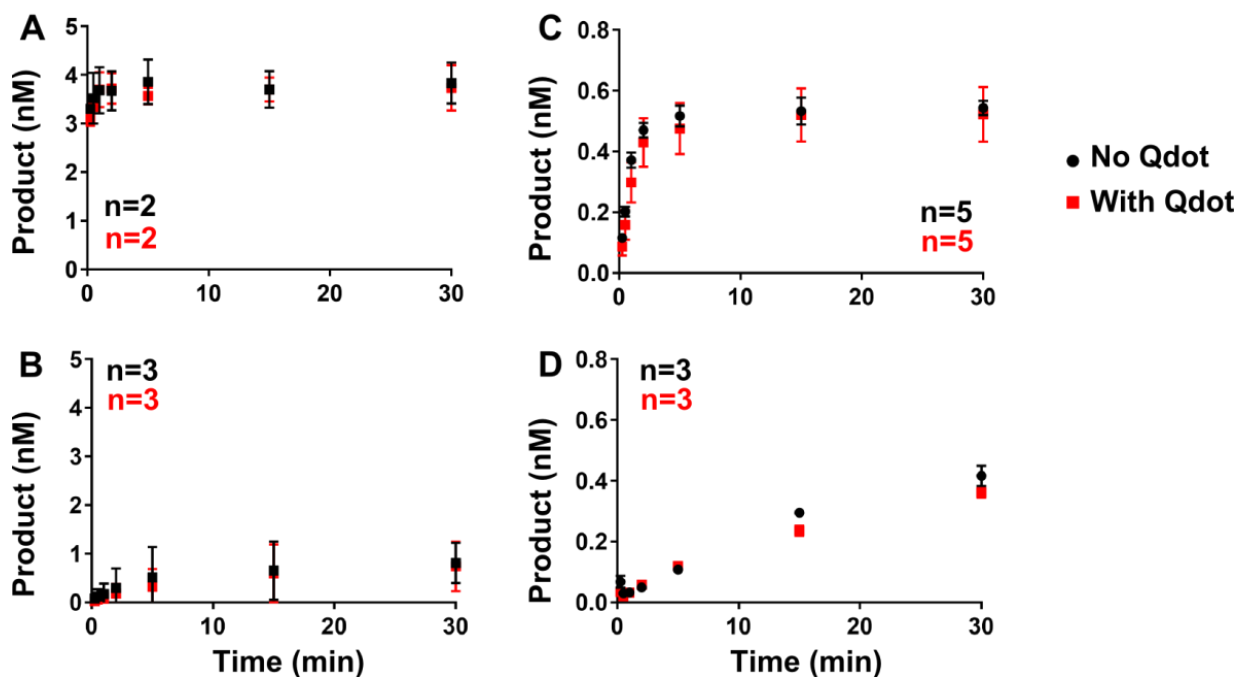


Fig. S11. Multiple turnover enzymatic activity of MUTYH WT and Y150C in the presence of Qdot. Gel-based assays monitor the rate of product generated by Qdot-labeled (red squares) and unlabeled (black circles) enzyme for (A) WT MutY, 4.6 nM total enzyme (B) MutY Y82C, 2 nM total enzyme (C) MUTYH WT, 4 nM total enzyme and (D) MUTYH Y150C, 4 nM total enzyme. All assays were in the presence of 20 nM 35-bp oligonucleotide containing an 8-oxoG:A mismatch. Number of replicates is shown in each graph. Error bars represent SEM and are within the data points if not visible.

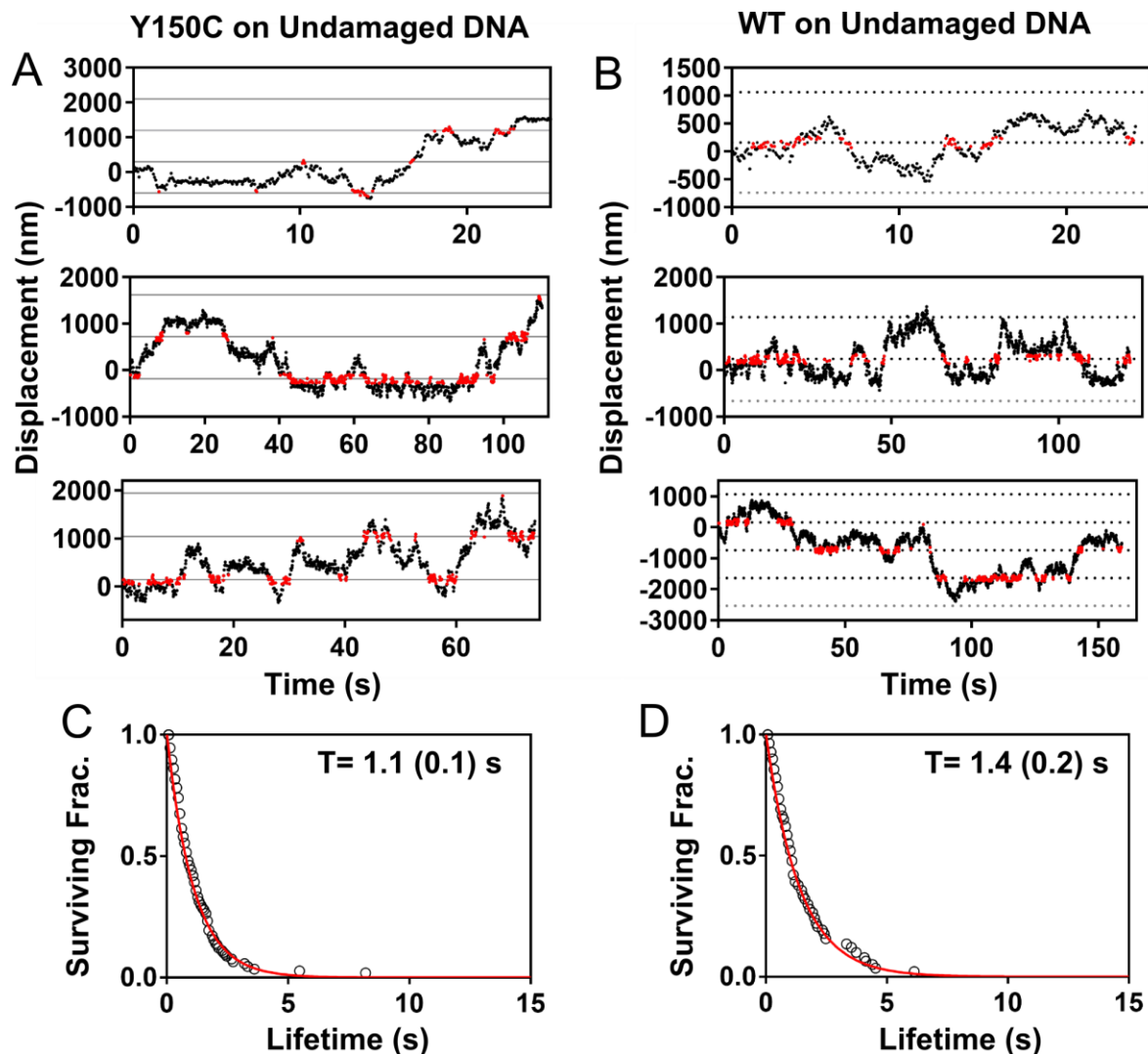


Fig. S12. Determination of transit lifetimes on undamaged DNA. A) Trajectories from Fig. 3A showing points within ± 100 nm of an undamaged location (red), 300nm away from the position localized 8-oxoG:A lesions. B) Representative trajectories of MUTYH WT on undamaged concatemer tightropes showing points ± 100 nm of a periodic, undamaged location (red) on the tightrope C) Lifetime distribution of MUTYH Y150C encounter lifetimes from panel A were fit with a double exponential model, but converged fit shows a single population with mean lifetime of 1.1 ± 0.1 s (131 encounter events over 5 trajectories, not all trajectories are shown). D) Lifetime distribution of MUTYH WT encounter lifetimes, fit as described above, and similarly, showing a single population with mean lifetime of 1.4 ± 0.2 s (70 encounter events over 3 trajectories).

Table S1. Diffusion constants and number of trajectories for each SM condition.

Enzyme	Substrate	Total Events	Number of Frames in D_{Time} Hist.	Number of Trajectories in D_{Time} Hist.	D_{Traj} ($\mu\text{m}^2\text{s}^{-1} \times 10^3$) ¹	Number of Trajectories to determine D_{Traj}	Total Tigtropes ²
MUTYH WT	lambda	88	10664	47	12.9 (2.2)	70	27
MUTYH Y150C	lambda	61	13939	43	14.5 (2.9)	56	25
MUTYH WT	rAP lambda	70	26330	61	0.979 (0.28)	65	20
MUTYH Y150C	rAP lambda	64	21883	46	6.33 (1.5)	50	16
MUTYH WT	Und pNIKCAT Cy5	79	64318	51	10.3 (2.5)	59	42
MUTYH Y150C	Und pNIKCAT Cy5	71	32166	33	11.7 (2.7)	49	30
MUTYH Y150A	Und pNIKCAT Cy5	39	25585	26	25.0 (6.9)	33	17
MUTYH WT	OG:A pNIKCAT Cy5	63	112199	59	0.155 (0.096)	63	36
MUTYH Y150C	OG:A pNIKCAT Cy5	84	47216	45	12.6 (3.8)	55	32
MUTYH Y150A	OG:A pNIKCAT Cy5	55	23623	33	10.1 (3.0)	39	18
MUTYH WT	OG:C pNIKCAT Cy5	80	80182	72	3.0 (1.0)	74	37
MUTYH Y150C	OG:C pNIKCAT Cy5	39	14227	22	8.4 (3.3)	24	20
MUTYH Y150A	OG:C pNIKCAT Cy5	26	14480	15	12.8 (5.0)	19	14
MutY WT	lambda	94	27819	73	14.0 (1.9)	88	36
MutY Y82C	lambda	93	2520	18	13.3 (1.8)	62	32
MutY WT	rAP lambda	71	18968	47	0.107 (0.049)	55	31
MutY Y82C	rAP lambda	55	8368	29	2.01 (0.87)	38	21

¹SEM is given in parentheses. ²Tigtropes vary in length from 3-20 μm and typically contain multiple damage sites.

References

1. Pope, M.A., Chmiel, N.H. and David, S.S. (2005) Insight into the functional consequences of hMYH variants associated with colorectal cancer: distinct differences in the adenine glycosylase activity and the response to AP endonucleases of Y150C and G365D murine MYH. *DNA Repair*, **4**, 315-325.
2. Dunn, A.R., Kad, N.M., Nelson, S.R., Warshaw, D.M. and Wallace, S.S. (2011) Single Qdot-labeled glycosylase molecules use a wedge amino acid to probe for lesions while scanning along DNA. *Nucleic Acids Res.*, **39**, 7487-7498.
3. Kow, Y.W. (1989) Mechanism of action of Escherichia coli exonuclease III. *Biochemistry*, **28**, 3280-3287.
4. Jorgensen, T.J., Kow, Y.W., Wallace, S.S. and Henner, W.D. (1987) Mechanism of Action of Micrococcus-Luteus Gamma-Endonuclease. *Biochemistry*, **26**, 6436-6443.
5. Bensimon, A., Simon, A., Chiffaudel, A., Croquette, V., Heslot, F. and Bensimon, D. (1994) Alignment and sensitive detection of DNA by a moving interface. *Science*, **265**, 2096-2098.
6. Allemand, J.F., Bensimon, D., Jullien, L., Bensimon, A. and Croquette, V. (1997) pH-dependent specific binding and combing of DNA. *Biophys. J.*, **73**, 2064-2070.
7. Nelson, S.R., Dunn, A.R., Kathe, S.D., Warshaw, D.M. and Wallace, S.S. (2014) Two glycosylase families diffusively scan DNA using a wedge residue to probe for and identify oxidatively damaged bases. *Proceedings of the National Academy of Sciences of the United States of America*.